



This is a repository copy of *Autonomous and reversible adhesion using elastomeric suction cups for in-vivo medical treatments*.

White Rose Research Online URL for this paper:

<https://eprints.whiterose.ac.uk/155481/>

Version: Accepted Version

Article:

Iwasaki, H., Lefevre, F., Damian, D. orcid.org/0000-0002-0595-0182 et al. (2 more authors) (2020) Autonomous and reversible adhesion using elastomeric suction cups for in-vivo medical treatments. *IEEE Robotics and Automation Letters*, 5 (2). pp. 2015-2022. ISSN 2377-3766

<https://doi.org/10.1109/LRA.2020.2970633>

© 2020 IEEE. Personal use of this material is permitted. Permission from IEEE must be obtained for all other users, including reprinting/ republishing this material for advertising or promotional purposes, creating new collective works for resale or redistribution to servers or lists, or reuse of any copyrighted components of this work in other works. Reproduced in accordance with the publisher's self-archiving policy.

Reuse

Items deposited in White Rose Research Online are protected by copyright, with all rights reserved unless indicated otherwise. They may be downloaded and/or printed for private study, or other acts as permitted by national copyright laws. The publisher or other rights holders may allow further reproduction and re-use of the full text version. This is indicated by the licence information on the White Rose Research Online record for the item.

Takedown

If you consider content in White Rose Research Online to be in breach of UK law, please notify us by emailing eprints@whiterose.ac.uk including the URL of the record and the reason for the withdrawal request.



eprints@whiterose.ac.uk
<https://eprints.whiterose.ac.uk/>

Autonomous and Reversible Adhesion using Elastomeric Suction Cups for In-vivo Medical Treatments

Haruna Iwasaki^{1,2}, Flavien Lefevre^{1,3}, Dana D. Damian⁴, Eiji Iwase², and Shuhei Miyashita^{1,4}

Abstract—Remotely controllable and reversible adhesion is highly desirable for surgical operations: it can provide the possibility of non-invasive surgery, flexibility in fixing a patch and surgical manipulation via sticking. In our previous work, we developed a remotely controllable, ingestible, and deployable pill for use as a patch in the human stomach. In this study, we focus on magnetically facilitated reversible adhesion and develop a suction-based adhesive mechanism as a solution for non-invasive and autonomous adhesion of patches. We present the design, model, and fabrication of a magnet-embedded elastomeric suction cup. The suction cup can be localised, navigated, and activated or deactivated in an autonomous way; all realised magnetically with a pre-programmed fashion. The use of the adhesion mechanism is demonstrated for anchoring and carrying, for patching an internal organ surface and for an object removal, respectively.

I. INTRODUCTION

Researchers strive for programmable medicine that enables an autonomous in vivo operation on targets such as ulcers or tumors. Microrobots and other programmable matter have been developed in the hope of providing the possible solutions. Researchers have proposed various types of functional microrobots and devices for in vivo use, such as micro-grippers or drug-delivering incision needles [1], [2], [3]. Providing smarter tools and devices that are practical, safe, and improve the surgical conduit is still a challenge. Another remaining challenge is the interface of such devices with tissue. One common interface is through adhesion, to apply a patch or attach a device.

Among the existing adhesion mechanisms, chemical adhesion glue is a widely used solution in medical surgeries [4], [5], [6], [7], [8]. However, their limitation is the existing trade off between the adhesion effectiveness and the biocompatibility of the adhesive. Outside the clinical setting, alternative approaches exist to name but a few, such as utilising the van der Waals force [9], [10], [11], surface tension [12], [13], [1], electrostatic force [14], or ice freezing [15]. However, these existing approaches require a physical access to the injury site and some are designed for single use and lack the autonomous operation.

The suction-based mechanism, typically achieved using a passive suction cup, is broadly used in daily life and shows a significant potential for fabrication as composite

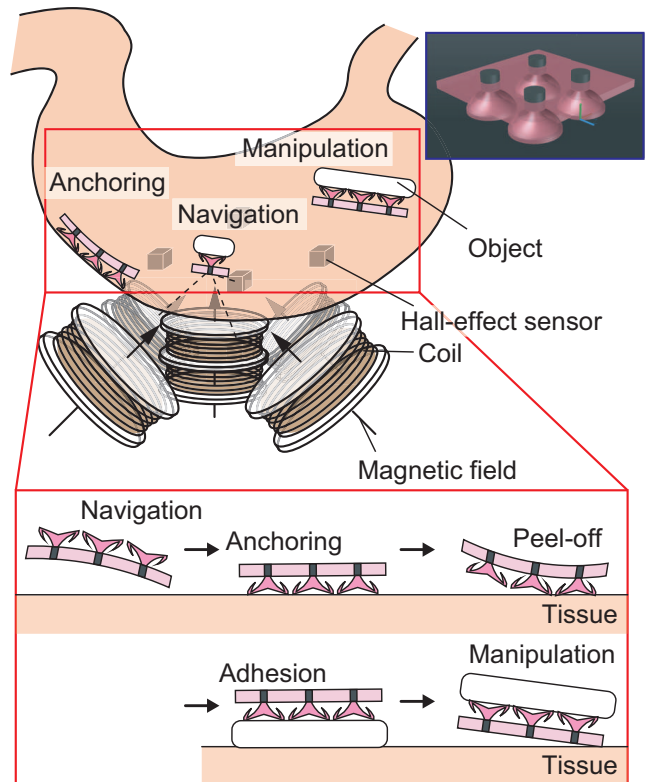


Fig. 1. The application scenario of remotely controllable elastomeric suction cup as a manipulator and a patch inside the stomach. The elastomeric suction cup is navigated and activated by an external magnetic field.

materials at a suitable scale [16], [17], [18], [19], [20], [21], although these existing suction cups use passive activation. It also shows promise as a tethered device in manipulation of endoluminal tissues [22], [23]. The adhesion achieved by a pressure cup is advantageous: it maintains its adhesion force without continuing to apply external force and enables repeated use. This means that it can be used as an engaging interface to manipulate objects via point-contact-based interaction, as a surgical remover to remove small lesions such as endoscopic mucosal resection (EMR), as an anchoring for a patch aiming at drug delivery, or sensor monitoring by fixation on an internal organ surface when multiple cups are placed on a surface.

Following our previous achievements in [24], [25] where a remotely controllable pill that can deploy, dress or plug, deliver a drug, and eventually biodegrade was presented, this study further advances the system by developing an autonomous suction-based adhesion mechanism for anchoring

¹Department of Electronic Engineering, University of York, Heslington, York, YO105DD, UK. ²Department of Applied Mechanics, Waseda University, Japan. haruna28@akane.waseda.jp ³Ecole Supérieure d'Electronique de l'Ouest, France. ⁴Department of Automatic Control and System Engineering, University of Sheffield, UK. Support for this work was provided by JASSO Japan Public-Private Partnership Student Study Abroad Program.

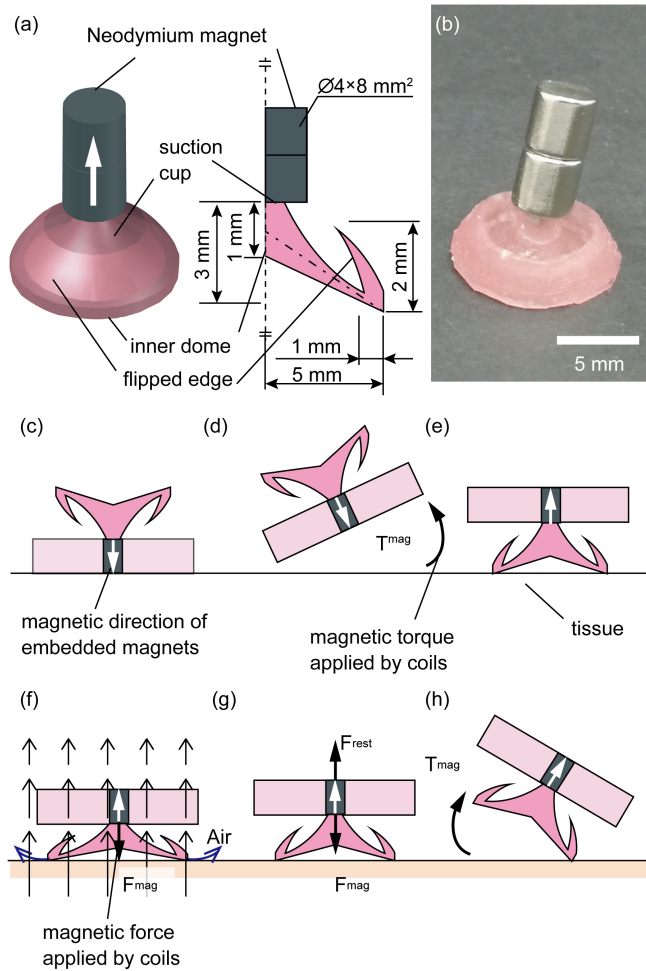


Fig. 2. The developed elastomeric suction cup and the actuation. (a) Schematics and (b) a fabricated suction cup. (c)-(h) Control of the suction cup. The white arrows in the magnets show the magnetic direction. The black bold arrows show the direction of magnetic force produced by the coils: (c) initial posture; (d) locomotion by wiggling using magnetic torque; (e) flipped state; (f) compression by magnetic force. The small arrows show the magnetic field gradient. (g) adhesion by restoring force of the material; (h) detachment by magnetic torque.

onto tissue and manipulating an object (Fig. 1). We also show the reversibility of the adhesion, which is a necessary feature for manipulation and for removal of a patch from the site. The control of the suction cup is managed with an electromagnetic coils, where the desired magnetic force and torque are realised with a superposed magnetic field. The contributions of this paper are:

- 1) Conception and composite fabrication of magnetically induced autonomous and reversible adhesion by an elastomer made suction cup.
- 2) Advanced shape design of suction cup to activate with lower external force, which is desirable for in-the-body use.
- 3) Demonstration of use as an anchor and a manipulator for a patch.

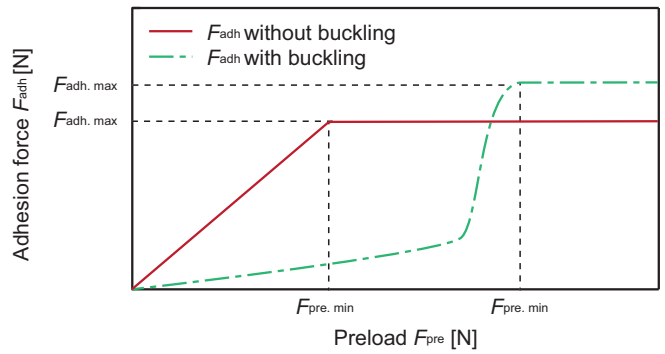


Fig. 3. Qualitative image of the relationship between preload and adhesion force of suction cups. When applying small preload, cups without buckling would adhere better than those with buckling while cups with buckling would adhere better when applying larger preload.

II. MATERIALS AND METHODS

A. Elastomeric Suction Cup Design

We newly designed an elastomeric suction cup which can be navigated and activated by an electromagnetic coil system (Fig. 1). The designed patch has one or more arrayed suction cups on its surface, which would realise autonomous and reversible adhesion onto curved surfaces such as stomach under dry and underwater condition.

In the case of remote activation using electromagnetic force, it is desired that the structure is activated with small external force to diminish the effect of the field on the human body. On the other hand, high adhesion force would be required after attaching to a target. Although existing suction cups, cups with positive curvature and thinner edge, have also achieved high adhesion force, those cups requires high preload to deform. Thus, we designed the suction cup with two unique features: negative curvature with varied cup thickness and a barb-like structure, called a Flipped edge, added to the ground contact edge of the cup (Fig. 2 (a) right). In order to reduce the external force necessary for activation, we designed the cup with a negative curvature with varied cup's thickness from the top to the bottom, which increases radial rigidity. The adhesion force using the suction cup is obtained by the pressure difference between the internal and external cup, which is occurred by the volume change of the internal cup when activated. Therefore, the bending rigidity in the vertical deformation is important parameter, which is affected by the buckling. The relationships between the preload F_{pre} and the adhesion force F_{adh} both with and without the buckling are shown in Fig. 3. Regardless of the buckling, F_{adh} is saturated when F_{pre} is above a preload (the maximum adhesion force $F_{adh,max}$ and minimum preload $F_{pre,min}$, respectively). It is because F_{adh} is occurred by the volume change.

However, when buckling occurs in the process up to $F_{adh,max}$, the volume change due to applying F_{pre} is non-linear, and therefore F_{adh} increases non-linearly. In this case, the deformed cup volume gradually decreases until the F_{pre} reaches the buckling load. Thus, the F_{adh} also increases gradually. When F_{pre} becomes more than the buckling load, the cup volume decreases drastically, and

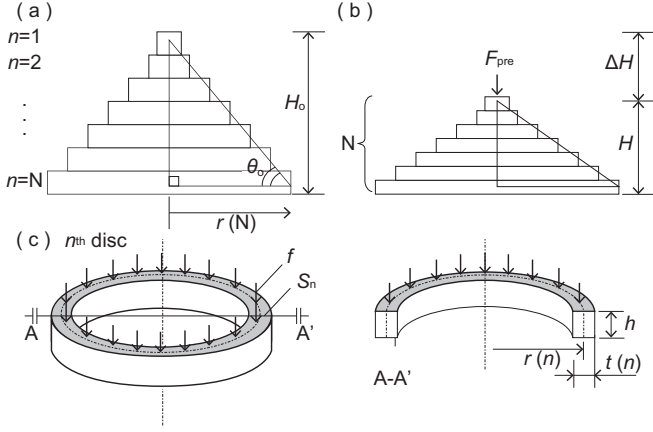


Fig. 4. Model of a suction cup. Side view of segmented suction cup in initial state (a) and compressed state (b). (c) Crossed view.

thus F_{adh} also increases drastically. On the other hand, when buckling does not occur, the volume change due to applying F_{pre} is linear, and therefore F_{adh} increases linearly towards $F_{adh,max}$. Thus, when activating with small preload F_{pre} , a cup without buckling would be desired for obtaining higher adhesion force. A cup with positive curvature could occur buckling, while a cup with negative curvature will be deformed linearly without buckling. Thus, we designed the cup with negative curvature that suppresses occurring buckling. Moreover, since the area contacting to the ground surface (contact zone) would relate to the adhesion force positively [26], we varied the thickness of the suction cup from the top to the bottom of the structure based on the following modelling so that the contact zone would be increased by propagating the external force uniformly. A suction cup is modelled as a stack of discs ($n \in 1, \dots, N$, numbered from the top to the bottom) as a bulk with linear region as shown in Fig. 4. Fig. 4(a) and (b) shows the initial state and activated state of the cup, respectively. The applied F_{mag} equates to the other reaction forces F_n . A suction cup is compressed vertically by the magnetic force, then deformed both vertically and horizontally. The relationship between the reaction force of the n -th structure element, F_n , and the cross-sectional area of the disc S_n is

$$F_n = k_n \Delta h_n = S_n f_n, \quad (1)$$

where k_n is the bending rigidity of the n_{th} disc, Δh_n is the height difference between the compressed and adhered cups, and f_n is force distribution of F_n . In order to propagate the external force uniformly, we assumed the the cross-sectional area, S_n , remains constant throughout the structure ($S_n = S_{n+1} = S_1$). The thickness of the n_{th} disc, $t(n)$, can be written as

$$t(n) = \frac{S_1}{2\pi r(n)}, \quad (2)$$

where $r(n)$ is the radius to the neutral axis of the disc. Moreover, $r(n)$ is written as

$$r(n) = \frac{n}{\tan \theta}, \quad (3)$$

where θ° is the radius the angle between the ground surface and the cup surface. Therefore, the ideal thickness variation is to decrease inversely with the number of the elements n , as shown in Fig. 4(e). With (3), (2) can be replaced by

$$t(n) = \frac{1}{n} \frac{S_1 \tan \theta}{2\pi}. \quad (4)$$

Based on (4), the thickness variation of the suction cup was designed. In our model, we obtain the thickness variation of the suction cup as $t(n) = 0.5 r(n)^{-1}$ where S_1 is $\pi \text{ mm}^2$. The flipped shape was designed and added to the ground contact edge in order to augment rigidity without suppressing the radial bending. As described in Section II-C-2, the cup with varied thickness was designed due to its activation. However, the thin bottom edge also causes the the vertical wavelike deformation, which enhances air leakage while adhering. Therefore, the cup should be designed with high circumferential rigidity related to vertical deformation at the bottom and low radial rigidity throughout the structure. Generally, according to beam theory, the bending moment M affecting to its section is defined as

$$M = \frac{EI}{\rho}, \quad (5)$$

where E is Young's modulus which depends on a material, I is the second moment of area, and ρ is the radius of curvature. EI is known as the bending stiffness. Thus, by increasing I , the bending will be suppressed. As shown in Fig. 4(c) by assuming that the cross-sectional piece is a rectangular shape, the relationship between the second moment of area I of and the its height h_n would be

$$I = \frac{t(n)h_n^3}{12}, \quad (6)$$

where $t(n)$ is width of the disc. Thus, increase in height $h(N)$ (vertical thickness of the cup at the bottom) would suppress the circumferential bending at the bottom. Furthermore, the flipped edge has a curved structure in order to maintain large adhesion area by bending inward, while the size of the structure has not been designed precisely.

B. Fabrication of the Arrayed Suction Cups

Fig. 5 shows the fabrication process of arrayed suction cups. The arrayed model consists of the multiple suction cups, a flexible elastomeric sheet and neodymium magnets. **Haruna: please check the following sentences** By multiplying suction cups, the adhesive performance of the device can be improved such. Even if some of the cups are detached, the rest of ones will keep adhered. Moreover, multiplying miniaturised suction cups will enable the sheet to adhere to curved surface. Four suction cups and a sheet are fabricated by molding using an elastomer, Ecoflex 00-30 A and B (Smooth On Inc.), mixed in a ratio of 1 : 1 by weight. Ecoflex 00-30 was chosen for prototyping owing to its wide availability and low cost. The uncured elastomer is mixed with a red food colouring in a beaker and degassed in a desiccator for 5 minutes to remove air bubbles. Then, the degassed elastomer is poured into a 3D printed (Connex3

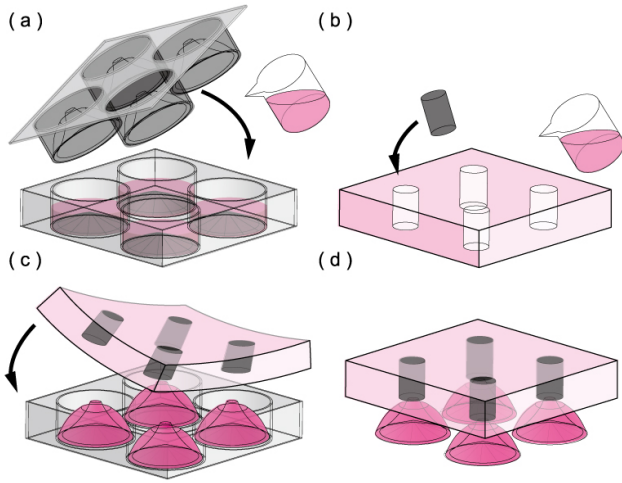


Fig. 5. The fabrication process for arrayed suction cups. (a) Ecoflex 00-30 is poured into a 3D printed template. Then, a lid is placed and left to cure. (b) Neodymium magnets are placed on an elastomeric sheet. (c) The sheet is attached to cured suction cups with glue. (d) Once dry, the suction cups are peeled away from the mould template.

Object 500, Stratasys) template with the shape of the inner surface of suction cups. A lid, whose surface has the shape of the outer surfaces of the suction cups, featuring Flipped edges, is pressed onto the mould template (Fig. 5 (a)). The template is placed in an oven for 5 min to cure the elastomer at 50°C. Then, cylindrical Neodymium magnets are attached to an elastomeric sheet fabricated using a 3D printed mould template (Fig. 5 (b)). The thickness of the centre of the sheet is the same as the magnet height (8 mm). The sheet must be light enough to enable to be pushed upward. In addition, the sheet must be wide enough: the distance from the edge of the sheet should be long enough to avoid undesired flipping instead of wiggling (Fig. 2(d)). Therefore, to make the device wider and lighter, the thickness of the edge of the sheet is designed to be thinner (3 mm) compared to the thickness near the middle. After curing the suction cups, the lid is removed and the sheet is attached to the suction cups with cyanoacrylates glue (Super Glue 5G, Loctite, Fig. 5 (c)). The glue was chosen owing to its availability but a silicone based glue is ideal for biocompatibility. To align the cups simultaneously, the sheet is attached before peeling the cups away from the template. Then, after curing the glue, the suction cups assembly is peeled off from the template (Fig. 5 (d)). Although this prototype is still large to ingest, we envisage rolling the sheet in order to make the assembly smaller [27]. In fact, researchers fabricate different-shaped elastomeric suction cups with 3D printed template [20], [21]. The producible size of suction cup mainly depends on the resolution of 3D printer. We estimate that the size can further be scaled down 30% by using a STL 3D printer.

C. Remote Actuation of Elastomeric Suction Cup

Fig. 2 (c)-(h) show the navigation and activation processes of suction cup. The suction cup has a 4mm×8mm ($\phi \times$ height) cylindrical magnet on top of its structure, and is thus navigated and activated by a magnetic field (Fig. 2 (d)

and Fig. 2 (f), respectively). An externally embedded Hall-effect sensor array detects the suction cup's location; thus, the system completes both locomotion and adhesion activation autonomously, without human intervention (see [25] for details of navigation). Further system information will be given in Section II-D. The suction cup is navigated with its non-adhesive side facing the surface of the tissue in order to avoid undesired adhesion. The navigation is realised using magnetic torque. Two alternating magnetic fields pointing at $\pm 45^\circ$ pitch angles are applied towards the direction of motion (Fig. 2 (d)). While navigating until reaching to the target object, the system repeated the following control cycle: (1) stop the application of magnetic field; (2) localise the magnet position using Hall-effect sensors; (3) update the magnet's path to the targeted location which position coordinates are pre-given; (4) apply a magnetic field to induce a motion of the patch. With using the sensors, the positions such as real-time location and targeted one are defined in X and Y coordinates. By repeating the cycle, the suction cup reaches the targeted location. When adherence is desired, the suction cup is flipped and then activated utilising a magnetic field gradient that produces a magnetic force (F_{mag}) so that an omnidirectional air flow is induced towards the outside of the cup (Fig. 2 (d)-(f)). When the magnetic force is released, the suction cup tends toward recovering its initial shape through restoring the force of the cup (restoring force). This deformation creates a negative pressure difference in the internal area between the cup and the substrate negative, which results in producing adhesive force. While adhering, the external magnetic field is absent, the restoring force is balanced out with the force occurred by the pressure difference **Haruna: former: adhesive force, which sounds better?** (Fig. 2 (g)). The adhesion would last while the pressure is kept negative.

Detachment is realised by inducing an air flow from outside of the suction cup and restoring the atmospheric pressure. Instead of pulling up from the edge by hands, we achieve this by applying a magnetic torque, causing deformation of the surface (Fig. 2 (h)). Since the adhesion force becomes lower when pulling up from its edge than when pulling up in vertical direction, the detachment is achieved by the magnetic torque. Owing to the restoring force, the suction cup can achieve repeatable adhesion.

D. Electromagnetic Control

The electromagnetic coil system consists of six coils: two horizontal coils (termed Top coil and Bottom coil; identified as $i \in 1, 2$ in the following equations) dedicated mainly to adhesion and detachment, and located under the workstage, and four coils dedicated to navigation and situated under the two horizontal coils. The latter four coils are inclined by 45° from the horizontal plane with cross-sectional faces oriented toward the centre of the workstage and identified as $i \in 3, \dots, 6$, in a clockwise order in the top view (see supporting material of [28] for details of control). The distance between neighboring inclined coils, the diameters of inclined and horizontal coils, and the distance between

the two horizontal coils are 250 mm, 130 mm, and 50 mm, respectively.

When the magnet on the suction cup is vertically oriented at the centre of the workstage with the estimated magnetic moment $m = 9.34 \times 10^{-2} \text{ Am}^2$, the magnetic force produced in a vertical direction ($F_{\text{mag.ver}}$), when 10 A are run through in each coil, can be estimated as

$$\begin{aligned} F_{\text{mag.ver}} &= \sum_{i=1}^2 F_{\text{mag}}^i + \sum_{i=3}^6 F_{\text{mag}}^i \\ &= 7.68 \times 10^{-3} + 2.14 \times 10^{-4} = 7.89 \times 10^{-3} \text{ N}. \end{aligned} \quad (7)$$

In the same way, when the same magnet is placed horizontally on the stage, the magnetic force produced in the horizontal direction ($F_{\text{mag.hor}}$) with the same amount of current when a magnet orients the same horizontal direction to the applied field is estimated as $1.07 \times 10^{-4} \text{ N}$. The magnetic forces are directly proportional to its size and number.

If arrayed suction cups are embedded in a structure and there exist multiple magnets, all the magnets experience the same magnetic field. However, owing to multiple magnets the Hall-effect sensors show a moderate inaccuracy in detecting the location precisely. For this reason, in our experiments, a suction cup was navigated and activated autonomously, while arrayed suction cups were navigated manually, with a visual feedback.

III. EXPERIMENTAL RESULTS

A. Adhesion Force Measurement

Fig.6 shows the experimental results of measuring the adhesion forces on a 1-mm-thick acrylic plate. We investigated the adhesion performances of four different structures shown in Fig.6 (a): a positive curved cup called Sphere, Cone, a negative curved cup with thickness variation (the internal angle is 25°) called Hat, and Hat with flipped edge. The adhesion forces with which the suction cups were activated by preloads with a force gauge (ZTA-5N, IMADA, 30 mm/min peel-off speed) were measured. The preload was applied instead of activating with magnetic force due to the wide range of preload. As shown in Fig.6 (b), throughout the experiments, we measured the tensile force from the time of applying the preload to the time of the detachment.

The maximum and minimum tensile force shown as adhesion force and its preload of each test, respectively are shown in Fig.6 (c). As shown in Fig.6 (c), the adhesion force of each structure tends to be increased as increasing preload, then saturated with a certain preload (the maximum adhesion force $F_{\text{adh.max}}$). We call the lowest preload to obtain the maximum adhesion force as the minimum preload $F_{\text{pre.min}}$. Flipped edge obtained the highest maximum adhesion force among the four structures as 0.9N, while Sphere obtained the lowest maximum adhesion force as 0.4N. There is an unique trend of the relationship between F_{pre} and F_{adh} . While Sphere has an inflection point, Hat and Flipped edge doesn't. As shown in Fig. 6 (b), the relationship between the displacement and F_{pre} also has similar trend. This indicates that for Sphere, the small deformation due to

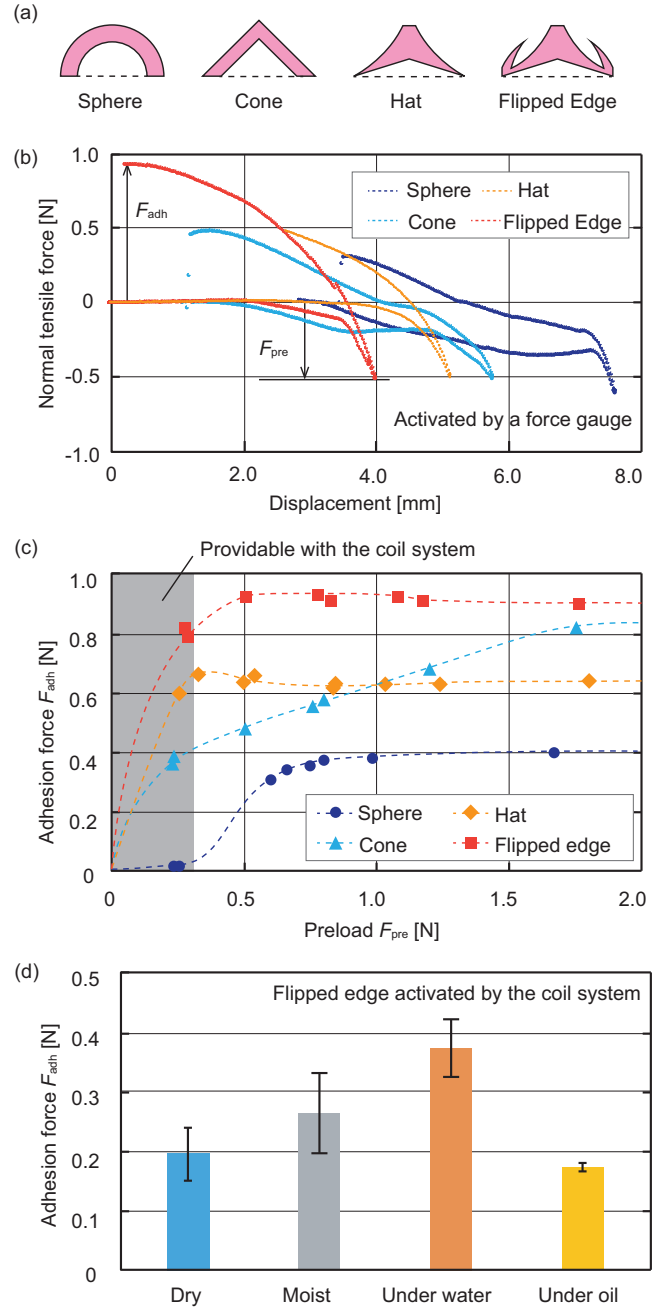


Fig. 6. Adhesion forces onto an acrylic plate with different suction cups. (a) Schematic cross view of four different suction shaped cups: Sphere, Pyramid, Hat, and Flipped edge. (b) Displacement dependency of the adhesion forces for the four different structures using a preload of 5 N on an acrylic plate in dry condition. (c) Adhesion forces of the four different structures using varied preloads from 0.25 N to 1.75 N on the acrylic plate in dry condition. (d) Adhesion forces of Flipped edge on the acrylic plate activated by magnetic force produced by the coils (the estimated magnetic moment $m = 9.34 \times 10^{-2} \text{ Am}^2$). Details of the experimental procedure are described in Section II-D).

the buckling suppressed adhering with small preload. The minimum preload depends on the structure, which both Flipped edge and Hat performed best ($F_{\text{pre.min}} = 0.3 \text{ N}$), then Cone and Sphere did in order. Especially, Sphere failed to adhere with lower than 0.3N preload but with over 0.5 N. In addition, for the lower preloads than each $F_{\text{pre.min}}$,

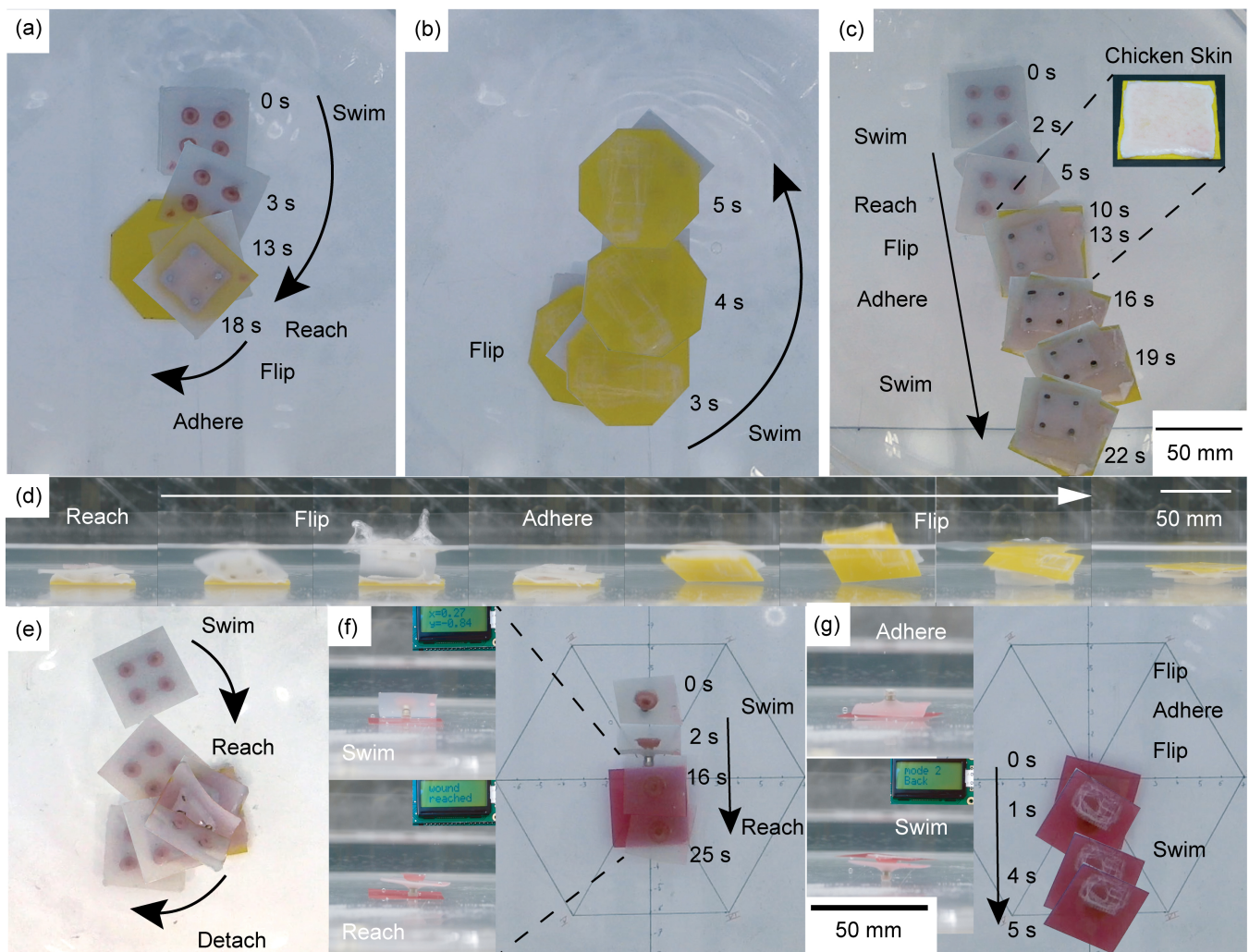


Fig. 7. Demonstration of autonomous adhesion. Arrayed suction cups were navigated manually, and a single suction cup was navigated autonomously. (a) A device with arrayed suction cups walks towards a target object (yellow acrylic plate), flips upside-down, and adheres to the object. (b) Then the device flips over again and walks away. (c) Another experiment where the device with arrayed suction cups adheres to and carries an animal tissue (chicken skin). It approaches a pre-determined location of the tissue, flips over, and adheres to it. It then walks away, carrying the tissue. (d) The side view of the experiment shown in (c). (e) The device was detached from the fixed animal tissue by applying magnetic torque. (f) The device walks towards a target object (red acrylic plate) through the autonomous navigation. The monitor on the top left shows the coordinates. (g) The device flips, adheres, and flips over again and walks away autonomously. See the supporting video for more details of the motions.

Flipped edge obtained the highest adhesion force, then Hat, Cone, and Sphere. Moreover, by comparing the adhesion force of Flipped edge with that of Hat, while the adhesion force of Flipped edge is higher than that of Hat by 0.25 N. As a result, by adding a thick edge, Flipped edge, the adhesion force was increased. Therefore, it is shown that Flipped edge would be the most suitable structure among the structures for the purpose activating by low preload on the coil system. We also confirmed the adhesion force of the most suitable shape, Flipped edge, to the acrylic plate, in dry, moisture, underwater, under oil condition as shown in Fig. 6(d). Among under the four conditions, the adhesion force underwater was the highest as 0.38 N, then under moist, dry, and under oil in particular order.

B. Manual Control of Suction Cup

The experiments with arrayed suction cups shown in Fig. 7(a)-(e) were conducted manually, by visually observing

the location of the device underwater. The other experiments using a single suction cup shown in Fig. 7(f) and (g) were autonomously achieved through magnetic localisation. Fig. 7(a)-(d) show two demonstrations in which arrayed suction cups were navigated and activated manually, and carried an acrylic plate (in (a) and (b)), and an animal tissue (chicken skin; in (c) and (d)). As target objects, a 1 mm-thick acrylic plate was used for the former demonstration, and a 2 mm-thick chicken skin glued to an acrylic plate was used for the latter. The directions of the magnetic field were switched periodically to induce walking motion of the arrayed suction cups. Then, the magnetic field was changed to a strong, constant, vertical magnetic field to flip and activate the arrayed suction cups. It took 18 s to reach the target object over a distance of approximately 15 mm distance. Once the reversed magnetic force is applied, the cups take a few seconds to adhere. The arrayed suction cups were flipped

again so that they would carry an object without bumping against the host organ's wall. Subsequently, the cups 'swam' back in the same mechanism as outbound movement using the opposite magnetic field direction. Fig. 7(e) shows the process of detachment of the arrayed suction cups from a fixed animal tissue (chicken skin). A rotational magnetic field of 28 mT alternating the orientations between -90° and 90° was applied and the produced magnetic torque caused the embedded magnets to align the magnetic direction by rotating upside down. Thus, the arrayed suction cups were peeled off. In addition, the arrayed suction cups kept adhering with its weight (13 g) to the acrylic plate in dry condition for XX minutes when the arrayed suction cups were activated by the coil system. Moreover, they kept adhering for 5 hours when it was activated with 0.5 N, which is the same preload as the demonstrations flipping and activating the arrayed suction cups. **Haruna: update once discussed**

C. Autonomous Control of Single Sction Cup

Fig. 7(f) and (g) show the demonstration of autonomously controlled navigation and transportation of a suction cup with a $30 \times 30 \times 0.5 \text{mm}^3$ acrylic plate. The suction cup was autonomously navigated to the location of the target object by having the system magnetically sense the location (Fig. 7(f)) once the location of the target object was pre-determined. Once a suction cup reached the target location, a vertical magnetic field was applied to flip the suction cup and trigger adhesion to the target. Once adhesion was completed, suction cup flipped with the object and swam away to the initial position autonomously (Fig. 7(g)). The process of reaching the object over a 50 mm distance was completed in 40 seconds.

IV. CONCLUSION

This study presented an autonomously reversible and remotely achieved adhesive mechanism, that is designed for use in non-invasive in vivo medicine. Adhesion utilises a suction mechanism; hence, it can be reversible and reusable. The suction cup proposed was newly designed, modelled, fabricated, and tested on the bench-top environment and with biological tissue. Its use with a single suction cup was demonstrated as an adhesive to anchor itself to a tissue and patch an area and as a carrier to manipulate an object, all in a fully autonomous fashion. The investigation of adhesion force indicates that the suction mechanism can be used for applications where the suction cups are activated autonomously under various medium conditions: dry, moist, underwater, and under oil. Further investigations with other conditions such as rough surfaces and material dependency remains for future work. The analyses and results show further potential of the mechanism to be scaled down and applied for various purposes in difficult-to-access locations at small scales and promising for in-the-body medical applications.

ACKNOWLEDGMENT

We thank Iain Will and Mark Hough for their technical support in this project.

REFERENCES

- [1] S. Yim, E. Gultepe, D. H. Gracias, and M. Sitti, "Biopsy using a magnetic capsule endoscope carrying, releasing, and retrieving untethered microgrippers," *IEEE Transactions on Biomedical Engineering*, vol. 61, no. 2, pp. 513–521, Feb 2014.
- [2] M. P. Kummer, J. J. Abbott, B. E. Kratochvil, R. Borer, A. Sengul, and B. J. Nelson, "Octomag: An electromagnetic system for 5-dof wireless micromanipulation," in *IEEE International Conference on Robotics and Automation (ICRA)*, May 3 - 8 2010, pp. 1006–1017.
- [3] S. Yang, E. o'cearbhaill, G. Sisk, K. M. Park, W. Cho, M. Villiger, B. Bouma, B. Pomahac, and J. Karp, "A bio-inspired swellable microneedle adhesive for mechanical interlocking with tissue," *Nature communications*, vol. 4, p. 1702, 2013.
- [4] N. Annabi, Y.-N. Zhang, A. Assmann, E. S. Sani, G. Cheng, A. D. Lassaletta, A. Vegh, B. Dehghani, G. U. Ruiz-Esparza, X. Wang, S. Gangadharan, A. S. Weiss, and A. Khademhosseini, "Engineering a highly elastic human protein-based sealant for surgical applications," *Science Translational Medicine*, vol. 9, no. 410, 2017.
- [5] J. Li, A. D. Celiz, J. Yang, Q. Yang, I. Wamala, W. Whyte, B. R. Seo, N. V. Vasilyev, J. J. Vlassak, Z. Suo, and D. J. Mooney, "Tough adhesives for diverse wet surfaces," *Science*, vol. 357, no. 6349, pp. 378–381, 2017.
- [6] N. Lang, M. J. Pereira, Y. Lee, I. Friehs, N. V. Vasilyev, E. N. Feins, K. Ablasser, E. D. O'Cearbhaill, C. Xu, A. Fabozzo, R. Padera, S. Wasserman, F. Freudenthal, L. S. Ferreira, R. Langer, J. M. Karp, and P. J. del Nido, "A blood-resistant surgical glue for minimally invasive repair of vessels and heart defects," *Science Translational Medicine*, vol. 6, no. 218, pp. 218ra6–218ra6, 2014.
- [7] H. Lee, N. F. Scherer, and P. B. Messersmith, "Single-molecule mechanics of mussel adhesion," *Proceedings of the National Academy of Sciences*, vol. 103, no. 35, pp. 12999–13003, 2006.
- [8] B. L. Walle, M. Gauthier, and N. Chaillet, "Dynamic modelling of a submerged freeze microgripper using a thermal network," in *2007 IEEE/ASME international conference on advanced intelligent mechatronics*, 4-7 Sept. 2007.
- [9] H. Lee, B. P. Lee, and P. B. Messersmith, "A reversible wet / dry adhesive inspired by mussels and geckos," *Nature Letters*, vol. 448, pp. 338–342, 2007.
- [10] A. G. Gillies, J. Kwak, and R. S. Fearing, "Controllable particle adhesion with a magnetically actuated synthetic gecko adhesive," *Advanced Functional Materials*, vol. 23, no. 16, pp. 3256–3261, 2013.
- [11] A. Mahdavi, L. Ferreira, C. Sundback, J. W. Nichol, E. P. Chan, D. J. D. Carter, C. J. Bettinger, S. Patanavanich, L. Chignozha, E. Ben-Joseph, A. Galakatos, H. Pryor, I. Pomerantseva, P. T. Masiakos, W. Faquin, A. Zumbuehl, S. Hong, J. Borenstein, J. Vacanti, R. Langer, and J. M. Karp, "A biodegradable and biocompatible gecko-inspired tissue adhesive," in *Proceedings of the National Academy of Sciences*, vol. 105, no. 7, 03 2008, pp. 2307–2312.
- [12] D.-M. Drotlef, M. Amjadi, M. Yunusa, and M. Sitti, "Bioinspired composite microfibers for skin adhesion and signal amplification of wearable sensors," *Advanced Materials*, vol. 29, no. 28, pp. 1701353–n/a, 2017.
- [13] J. Giltinan, E. Diller, and M. Sitti, "Programmable assembly of heterogeneous microparts by an untethered mobile capillary microgripper," *Lab Chip*, vol. 16, pp. 4445–4457, 2016.
- [14] M. Graule, P. Chirattananon, S. Fuller, N. T. Jafferis, K. Y. Ma, M. Spenko, R. Kornbluh, and R. J. Wood, "Perching and takeoff of a robotic insect on overhangs using switchable electrostatic adhesion," *Science*, vol. 352, pp. 978–982, 2016.
- [15] S. Miyashita, F. Casanova, M. Lungarella, and R. Pfeifer, "Peltier-based freeze-thaw connector for waterborne self-assembly systems," in *2008 IEEE/RSJ International Conference on Intelligent Robots and Systems*, Sep. 2008, pp. 1325–1330.
- [16] M. K. Choi, O. K. Park, C. Choi, S. Qiao, R. Ghaffari, J. Kim, D. J. Lee, M. Kim, W. Hyun, S. J. Kim, H. J. Hwang, S.-H. Kwon, T. Hyeon, N. Lu, and D.-H. Kim, "Cephalopod-inspired miniaturized suction cups for smart medical skin," *Advanced Healthcare Materials*, vol. 5, no. 1, pp. 80–87, 2016.

- [17] S. Baik, D. W. Kim, Y. Park, T.-J. Lee, S. H. Bhang, and C. Pang, "A wet-tolerant adhesive patch inspired by protuberances in suction cups of octopi," *Nature*, vol. 546, no. 7658, pp. 396–400, June 2017.
- [18] S. Song, D.-M. Drotlef, C. Majidi, and M. Sitti, "Controllable load sharing for soft adhesive interfaces on three-dimensional surfaces," in *Proceedings of the National Academy of Sciences*, vol. 114, no. 22, 2017, pp. E4344–E4353.
- [19] H. Lee, D.-S. Um, Y. Lee, S. Lim, H.-j. Kim, and H. Ko, "Octopus-inspired smart adhesive pads for transfer printing of semiconducting nanomembranes," *Advanced Materials*, vol. 28, no. 34, pp. 7457–7465, 2016.
- [20] R. Manabe, K. Suzumori, and S. Wakimoto, "A functional adhesive robot skin with integrated micro rubber suction cups," in *2012 IEEE International Conference on Robotics and Automation*, May 2012, pp. 904–909.
- [21] S. Lee, H. Kim, W. Lee, and J. Kim, "Finger-triggered portable pdms suction cup for equipment-free microfluidic pumping," *Micro and Nano Systems Letters*, vol. 6, no. 1, p. 1, Mar 2018.
- [22] T. Ranzani, S. Russo, C. J. Walsh, and R. J. Wood, "A soft suction-based end effector for endoluminal tissue manipulation," in *The 9th Hamlyn Symposium on Medical Robotics*, 27 June 2016.
- [23] S. Becker, T. Ranzani, S. Russo, and R. J. Wood, "Pop-up tissue retraction mechanism for endoscopic surgery," in *2017 IEEE/RSJ International Conference on Intelligent Robots and Systems, IROS 2017*, 24–28 September 2017, pp. 920–927.
- [24] S. Miyashita, S. Guitron, K. Yoshida, S. Li, D. D. Damian, and D. Rus, "Ingestible, controllable, and degradable origami robot for patching stomach wounds," in *2016 IEEE International Conference on Robotics and Automation (ICRA)*, 2016, pp. 909–916.
- [25] A. Du Plessis D'Argent, S. Perry, Y. Iwata, H. Iwasaki, I. Will, A. Fabozzo, E. Iwase, D. Rus, D. Damian, and S. Miyashita, "Programmable medicine: Autonomous, ingestible, deployable patch and plug for stomach ulcer therapy," in *2018 IEEE International Conference on Robotics and Automation (ICRA)*, 21–25 May 2018, pp. 1511–1518.
- [26] D. Ge, T. Matsuno, Y. Sun, C. Ren, Y. Tang, and S. Ma, "Quantitative study on the attachment and detachment of a passive suction cup," *Vacuum*, vol. 116, pp. 13 – 20, 2015.
- [27] Y. Iwata, S. Miyashita, and E. Iwase, "Self-rolling up micro 3d structures using temperature-responsive hydrogel sheet," *Journal of Micromechanics and Microengineering*, vol. 27, no. 12, p. 124003, 2017.
- [28] S. Miyashita, S. Guitron, S. Li, and D. Rus, "Robotic metamorphosis by origami exoskeletons," *Science Robotics*, vol. 2, no. 10, p. eaao4369, 2017.